

Combination of Sustained Off-Resonance Irradiation and On-Resonance Excitation in FT-ICR

Kristin A. Herrmann,[†] Árpád Somogyi,[†] Vicki H. Wysocki,[†] László Drahos,[‡] and Károly Vékey^{*,‡}

Department of Chemistry, University of Arizona, Tucson, Arizona 85721, and Institute of Chemistry, Chemical Research Center of the Hungarian Academy of Sciences, H-1025, Pusztaszeri u. 59-67, Budapest, Hungary

Fourier transform ion cyclotron resonance (FT-ICR) mass spectrometry is becoming more widely used among the mass spectrometric techniques and has excellent figures of merit. Ion activation and fragmentation via sustained off-resonance irradiation (SORI) collision-induced dissociation (CID) is commonly used in FT-ICR. However, one of the limitations of SORI-CID is that only low-energy processes are typically observed in the product ion spectra. Here we present another option for performing CID in FT-ICR, a combination of SORI and on-resonance excitation (RE), termed SORI-RE. In comparison to SORI, this method produces more abundant ions resulting from higher energy fragmentation pathways. The result is the observation of a significant abundance of both higher and lower energy fragmentation pathways in the same mass spectrum. The comparison of SORI, RE, and SORI-RE spectra may lead to mechanistic insights as the relative abundances of certain fragment ions change as a function of internal energy deposition. This technique is simple to incorporate in existing instruments, does not require hardware or software modification, and requires only an additional 20–40 ms acquisition time. The technique is illustrated for a peptide (YGGFL), two disaccharides differing in the position of the glycosidic linkage (2 α -mannobiose, 3 α -mannobiose), an oligosaccharide (Alditol XT), a small protein (ubiquitin), and an inorganic cation (UO₂⁺). Examples of higher energy fragmentation pathways enhanced by SORI-RE include the formation of immonium ions and oligosaccharide cross-ring cleavages.

Fourier transform ion cyclotron resonance (FT-ICR) mass spectrometry (MS) is a well-established high-resolution and accurate mass technique that can be successfully applied in single- and multiple-stage (MSⁿ) modes to gain sequence and structural information about biopolymers such as proteins, peptides, and carbohydrates.^{1,2} FT-ICR is routinely coupled to matrix-assisted laser desorption/ionization (MALDI)³ and electrospray ionization⁴ (ESI) for the study of large biomolecules.

Ion dissociation techniques for the fragmentation of biomolecules in FT-ICR include infrared multiphoton dissociation (IRMPD),^{5–7} blackbody infrared radiative dissociation (BIRD),^{8,9} sustained off-resonance irradiation collision-induced dissociation (SORI-CID),^{10,11} on-resonance excitation CID (RE-CID),^{12–14} electron capture dissociation (ECD),^{15–17} surface-induced dissociation (SID),^{18,19} electron detachment dissociation (EDD),²⁰ and UV photodissociation.^{21–23} Information about the primary structure of a biomolecule is obtained through sequence-specific fragmentation. This includes fragmentation between basic building blocks, such as amino acid residues, and fragment ions characteristic of building blocks (i.e., amino acid immonium ions, which define the presence of a corresponding amino acid in a peptide and can be used to eliminate candidate sequences during peptide identi-

- (3) Karas, M.; Hillenkamp, F. *Anal. Chem.* **1988**, *60*, 2299–2301.
- (4) Fenn, J. B.; Mann, M.; Meng, C. K.; Wong, S. F.; Whitehouse, C. M. *Science* **1989**, *246*, 64–71.
- (5) Zhang, J. H.; Schuboth, K.; Li, B. S.; Russell, S.; Lebrilla, C. B. *Anal. Chem.* **2005**, *77*, 208–214.
- (6) Woodin, R. L.; Bomse, D. S.; Beauchamp, J. L. *J. Am. Chem. Soc.* **1978**, *100*, 3248–3250.
- (7) Little, D. P.; Speir, J. P.; Senko, M. W.; Oconnor, P. B.; McLafferty, F. W. *Anal. Chem.* **1994**, *66*, 2809–2815.
- (8) Dunbar, R. C.; McMahon, T. B. *Science* **1998**, *279*, 194–197.
- (9) Price, W. D.; Schnier, P. D.; Williams, E. R. *Anal. Chem.* **1996**, *68*, 859–866.
- (10) Senko, M. W.; Speir, J. P.; McLafferty, F. W. *Anal. Chem.* **1994**, *66*, 2801–2808.
- (11) Gauthier, J. W.; Trautman, T. R.; Jacobson, D. B. *Anal. Chim. Acta* **1991**, *246*, 211–225.
- (12) Cody, R. B.; Burnier, R. C.; Cassady, C. J.; Freiser, B. S. *Anal. Chem.* **1982**, *54*, 2225–2228.
- (13) Cody, R. B.; Freiser, B. S. *Anal. Chem.* **1982**, *54*, 1431–1433.
- (14) Cody, R. B.; Burnier, R. C.; Freiser, B. S. *Anal. Chem.* **1982**, *54*, 96–101.
- (15) McLafferty, F. W.; Horn, D. M.; Breuker, K.; Ge, Y.; Lewis, M. A.; Cerda, B.; Zubarev, R. A.; Carpenter, B. K. *J. Am. Soc. Mass Spectrom.* **2001**, *12*, 245–249.
- (16) Zubarev, R. A.; Horn, D. M.; Fridriksson, E. K.; Kelleher, N. L.; Kruger, N. A.; Lewis, M. A.; Carpenter, B. K.; McLafferty, F. W. *Anal. Chem.* **2000**, *72*, 563–573.
- (17) Zubarev, R. A.; Kelleher, N. L.; McLafferty, F. W. *J. Am. Chem. Soc.* **1998**, *120*, 3265–3266.
- (18) Laskin, J.; Denisov, E.; Futrell, J. H. *Int. J. Mass Spectrom.* **2002**, *219*, 189–201.
- (19) Chorush, R. A.; Little, D. P.; Beu, S. C.; Wood, T. D.; McLafferty, F. W. *Anal. Chem.* **1995**, *67*, 1042–1046.
- (20) Budnik, B. A.; Haselmann, K. F.; Zubarev, R. A. *Chem. Phys. Lett.* **2001**, *342*, 299–302.
- (21) Williams, E. R.; Furlong, J. J. P.; McLafferty, F. W. *J. Am. Soc. Mass Spectrom.* **1990**, *1*, 288–294.
- (22) Hunt, D. F.; Shabanowitz, J.; Yates, J. R. *J. Chem. Soc., Chem. Commun.* **1987**, 548–550.
- (23) Bowers, W. D.; Delbert, S. S.; McIver, R. T. *Anal. Chem.* **1986**, *58*, 969–972.

* To whom correspondence should be addressed. E-mail: vekey@chemres.hu. Phone: 36-1-438-0481. Fax: 36-1-325-9105.

[†] University of Arizona.

[‡] Chemical Research Center of the Hungarian Academy of Sciences.

(1) Amster, I. J. *J. Mass Spectrom.* **1996**, *31*, 1325–1337.

(2) Hakansson, K.; Cooper, H. J.; Hudgins, R. R.; Nilsson, C. L. *Curr. Org. Chem.* **2003**, *7*, 1503–1525.

fication searches). This fragmentation should be as nonselective as possible to maximize the structural information gained. IRMPD, BIRD, and SORI-CID can be considered “gentle” ion activation techniques and are characterized by fragment ions resulting mainly from low-energy processes. SORI-CID and RE-CID are analogous fragmentation techniques differing in application by the frequency, amplitude, and time of the energy pulse applied to translationally excite the ions.

During SORI-CID, ions are excited by application of an rf electric field pulse with a frequency “off-resonance” with the ion’s natural cyclotron frequency, ω_c . This frequency pulse results in a maximum translational energy, E_{tr} , given by

$$E_{tr} = (E/\sqrt{2})^2 e^2 / [2m(\omega - \omega_c)^2] \sin^2(\omega - \omega_c)t/2 \quad (1)$$

where E is the amplitude of the rf pulse, e is the electric charge, ω is the excitation frequency, and t is the duration of the rf pulse.^{11,24} The “off-resonance” pulse results in the ion undergoing some number, n , of acceleration–deceleration cycles given by²⁴

$$n = t(\omega - \omega_c) \quad (2)$$

A result of these acceleration–deceleration cycles is that an ion will be confined in the cell for a sustained period of irradiation (>500 ms). In the presence of a low-mass gas target (e.g., N_2 or Ar) at a pressure of $\sim 10^{-6}$ Torr, SORI results in many sequential, low-energy inelastic collisions, which activates the molecules slowly. This “slow activation” results in dissociation occurring mainly through the lowest energy fragmentation channels.^{11,25}

Fragmentation in an FT-ICR cell can also be accomplished by applying a short (<500 μ s) rf pulse whose frequency is *on-resonance* (termed RE for on-resonance excitation) with the cyclotron frequency of the ion (e.g., $\omega = \omega_c$). In this case, the maximum translational energy of the ion is given by^{11,26}

$$E_{tr} = (E/\sqrt{2})^2 e^2 t^2 / 8m \quad (3)$$

The formation of ions off-axis is a disadvantage of RE-CID resulting in a radial, diffusional loss of product ions, limited subsequent stages of fragmentation, and reduced resolving power.²⁷ RE is, in practice, more time-consuming to optimize than SORI. These shortcomings have led to SORI-CID as the preferred method of fragmentation, although RE-CID excitation is sometimes more efficient at producing ions resulting from higher energy fragmentation pathways.

In certain instances, it is advantageous from structural and analytical points of view to obtain fragment ions resulting from both low- and high-energy fragmentation pathways. However, certain fragmentation pathways may be particularly facile when a low-energy, slow-heating collisional activation technique such as SORI-CID is used, causing higher energy pathways to be suppressed.¹¹ This is especially true in the fragmentation of carbo-

hydrates in which the cleavage of the glycosidic linkages occurs generally at lower fragmentation thresholds and cross-ring cleavages occur at higher fragmentation thresholds. Another example is the fragmentation of protonated peptides. Statistical analyses and mechanistic studies of peptide fragmentation have revealed residue-specific preferential cleavage N-terminal to proline (Pro) in the presence of a mobile proton and C-terminal to aspartic acid (Asp) and glutamic acid (Glu) in the absence of a mobile proton.^{28–36} Under certain conditions, the dominance of these preferential cleavages may lead to a loss of fragmentation information because other fragment peaks may be of very low abundance or not present.

Here, we introduce the combination of SORI-CID and RE-CID, termed SORI-RE, which often enhances the observation of higher energy fragmentation product ions. In SORI-RE, a SORI pulse is followed by a comparatively short RE pulse. The application of the SORI pulse increases the internal energy of the ions so that some portion of the ions has enough internal energy to dissociate, mainly through the lowest energy dissociation pathways. The undissociated but activated ions remain below the fragmentation threshold. The subsequent application of a RE pulse causes the internal energy of the remaining precursor ions to rise significantly above the fragmentation threshold. This results in an enhancement of higher energy fragment ions, which appear along with the lower energy fragment ions produced in the SORI step. In certain instances, the ion population is not homogeneous, but exists as a heterogeneous mixture with several subpopulations containing different protonated forms or conformations, as demonstrated by ion mobility and gas-phase H/D exchange.^{37–39} The increased internal energy produced in SORI-RE does not simply initiate higher energy fragmentation but may also alter these heterogeneous populations. The experiment described here is related to a so-called “pump–probe” experiment, described before.⁴⁰ In the previous experiment, BIRD was used to raise the internal energy of the precursor ion to a well-defined value. Next, RE-CID was used to probe the amount of additional energy needed to reach a particular, final internal energy distribution. In the present experiment, SORI is used to pump energy into the precursor ion so that some portion of the precursor ions fragment through low-energy pathways and RE is used to induce higher

(24) Beauchamp, J. L. *Annu. Rev. Phys. Chem.* **1971**, *22*, 527–561.

(25) McLuckey, S. A.; Goeringer, D. E. *J. Mass Spectrom.* **1997**, *32*, 461–474.

(26) Grosshans, P. B.; Marshall, A. G. *Int. J. Mass Spectrom. Ion Processes* **1990**, *100*, 347–379.

(27) Guan, S. H.; Marshall, A. G.; Wahl, M. C. *Anal. Chem.* **1994**, *66*, 1363–1367.

(28) Brei, L. A.; Tabb, D. L.; Yates, J. R.; Wysocki, V. H. *Anal. Chem.* **2003**, *75*, 1963–1971.

(29) Huang, Y. Y.; Wysocki, V. H.; Tabb, D. L.; Yates, J. R. *Int. J. Mass Spectrom.* **2002**, *219*, 233–244.

(30) Grewal, R. N.; El Aribi, H.; Harrison, A. G.; Siu, K. W. M.; Hopkinson, A. C. *J. Phys. Chem. B* **2004**, *108*, 4899–4908.

(31) Gu, C. G.; Tsaprailis, G.; Brei, L.; Wysocki, V. H. *Anal. Chem.* **2000**, *72*, 5804–5813.

(32) Tsaprailis, G.; Somogyi, Á.; Nikolaev, E. N.; Wysocki, V. H. *Int. J. Mass Spectrom.* **2000**, *196*, 467–479.

(33) Wattenberg, A.; Organ, A. J.; Schneider, K.; Tyldesley, R.; Bordoli, R.; Bateman, R. H. *J. Am. Soc. Mass Spectrom.* **2002**, *13*, 772–783.

(34) Leymarie, N.; Berg, E. A.; McComb, M. E.; O’Connor, P. B.; Grogan, J.; Oppenheim, F. G.; Costello, C. E. *Anal. Chem.* **2002**, *74*, 4124–4132.

(35) Yu, W.; Vath, J. E.; Huberty, M. C.; Martin, S. A. *Anal. Chem.* **1993**, *65*, 3015–3023.

(36) Qin, J.; Chait, B. T. *J. Am. Chem. Soc.* **1995**, *117*, 5411–5412.

(37) Frietas, M.; Hendrickson, C. L.; Emmett, M. R.; Marshall, A. G. *J. Am. Soc. Mass Spectrom.* **1998**, *9*, 1012–1019.

(38) Valentine, S. J.; Clemmer, D. E. *J. Am. Chem. Soc.* **1997**, *119*, 3558–3566.

(39) Herrmann, K. A.; Wysocki, V. H.; Vorpagel, E. R. *J. Am. Soc. Mass Spectrom.* **2005**, *16*, 1067–1080.

(40) Heeren, R. M. A.; Vékey, K. *Rapid Commun. Mass Spectrom.* **1998**, *12*, 1175–1181.

energy fragmentation of the remaining activated ion population. The internal energy is more well-defined in BIRD than in SORI, and so BIRD-RE is therefore more appropriate for fundamental energy deposition studies. However, the SORI-RE experiment represents a practical method for the enhancement of fragment ions resulting from higher energy pathways. This technique is both rapid and easy to apply in existing FT-ICR instruments equipped to perform SORI-CID because no hardware or software modification is required and the acquisition time is increased by only 20–40 ms. The information SORI-RE provides is complementary to SORI alone and can also provide additional structural/mechanistic information.

EXPERIMENTAL SECTION

Alditol XT, an O-linked oligosaccharide isolated from frog egg jelly,⁵ was provided by the Carlito Lebrilla research group at the University of California, Davis. Uranyl nitrate hexahydrate was purchased from Aldrich (St. Louis, MO) and recrystallized before use. Methanol was purchased from J. T. Baker (Phillipsburg, NJ) and used as received. The 18-M Ω Milli-Q water was prepared (Millipore Corp., Bedford MA). All other chemicals were purchased from Sigma-Aldrich (St. Louis, MO) and used without further purification.

An IonSpec (Lake Forest, CA) 4.7-T FT-ICR instrument was used for all fragmentation studies. Ions were generated using an Analytica (Branford, CT) second-generation ESI source. All samples were introduced into the instrument by infusion at a flow rate of 2–3 μ L/min through a stainless steel microelectrospray needle (0.004-in. i.d.). Leucine enkephalin and ubiquitin solutions were prepared at a concentration of \sim 10–30 μ M in 1:1 methanol/water with 1% acetic acid. 2 α -Mannobiose and 3 α -mannobiose were prepared in a similar manner, except Li₂CO₃ was added at a concentration of \sim 30 μ M to induce formation of the lithiated molecules. Alditol XT was prepared at a concentration of 10–30 μ M in 1:1 methanol/water. The sodiated alditol XT ion was the main ion observed, although sodium ions were not added to the solution. Solutions 1 mM in UO₂²⁺ and 2 mM in NO₃⁻ were prepared in water and diluted 3-fold with 2:1 methanol/water. The glass capillary temperature was kept at 60 °C, and 3.8 kV was applied to the electrospray needle.

The electrosprayed ions pass through a skimmer and are collected in an external rf-only hexapole, where they are allowed to accumulate for 300–1000 ms before being passed into the analyzer through a shutter. An rf-only quadrupole guides the ions into the cylindrical ICR cell. Once the precursor ions are trapped inside the ICR cell, all other mass-to-charge values are ejected from the cell via a frequency sweep isolating the desired ion. Monoisotopic isolation was used for this study (except for ubiquitin) because RE tends to deplete the monoisotopic precursor ion peak (especially for singly charged precursor ions) while SORI may excite the ¹³C isotopic ion (with a +1000-Hz offset, for example). The absolute signal intensity of the precursor ion after isolation varied by less than \pm 10% when electrospray conditions were kept constant. After isolation, fragmentation was accomplished by SORI, RE, SORI-RE, or RE-SORI. SORI pulses varied in time from 50 to 3000 ms and SORI voltages varied from 0.5 to 6.0 V. Likewise, RE pulses varied in time from 10 to 25 μ s, and RE voltages varied from 50 to 400 V. Either nitrogen or argon gas was used as the collision gas at a pressure of \sim 2 \times 10⁻⁶ Torr

in the ICR cell. The gas pulse was controlled through a pulse valve held open for the desired amount of time. For all SORI-CID experiments, the gas pulse started with the beginning of the SORI pulse and was applied for the same duration as the SORI pulse plus 50 ms. The SORI offset frequency was +1000 Hz. Changing the offset polarity had no observable effect on spectral appearance. As expected, as absolute offset frequency was reduced, the spectrum became more similar to a RE spectrum. For all RE-CID experiments, a RE pulse was applied 20 ms (minimum gap time required by hardware) after a 0 V “blank” SORI pulse. In addition, the gas was pulsed into the cell at the same time and for 50 ms longer than the 0 V blank SORI pulse (i.e., 550 ms total gas pulse). For all SORI-RE experiments, the gas pulse started with the beginning of the SORI pulse and ended 50 ms after the end of the SORI pulse. For all RE-SORI experiments, the gas pulse started 500 ms before the RE pulse and ended with the end of the SORI pulse. During the SORI-RE experiments, the RE pulse was applied 20 ms after the end of the SORI pulse. In a few additional experiments, the time gap between SORI and RE (and also between RE and SORI) was varied between 20 and 500 ms.

An rf sweep with a width of 2 ms and amplitude of 120 V was used to excite the ions before detection. Broadband detection with an ADC rate of 2 MHz and 512K samples was used. Three spectra were collected for each data point during the systematic measurement of the effect of SORI and RE time and amplitude on the fragmentation of leucine enkephalin. The B-spline standard routine in the Origin graphing software was used to connect the points. All spectra shown are the result of one acquisition; however, the acquisition was repeated at least three times to ensure reproducibility. Variation in ion abundances was generally less than \pm 10%.

Theoretical modeling has been performed by the MassKinetics 1.5 software program.⁴¹ This is a reaction kinetic model based on RRKM rate theory and has been described elsewhere.⁴² The program uses known experimental parameters (e.g., voltages, time scales, and gas pressure), calculated molecular parameters (e.g., vibrational frequencies as calculated quantum mechanically at the B3LYP 6-31 G* level), and reaction parameters such as critical energy and preexponential factors. To model fragmentation of leucine enkephalin, the well-known fragmentation scheme of peptides was used.⁴³ The preexponential factor and critical energy corresponding to leucine enkephalin b₄ ion formation was used as measured experimentally.⁴⁴ To avoid overfitting, a simple fragmentation model with a minimum number of adjustable parameters was used. All preexponential factors were 10¹¹, which is close to the value for b₄ formation. Critical energies for the formation of a₄, b₃, y₂, and Y (equal to F) and for the mean collisional energy-transfer value were optimized, altogether five adjustable parameters. The optimization criterion was to yield minimum root-mean-square error between calculated and experimentally determined SORI, RE, and SORI-RE spectra. Identical parameters were used to calculate energy distributions, and time- and energy-dependent SORI, RE, and SORI-RE spectra. Using additional adjustable parameters, such as optimizing the pre-

(41) Drahos, L.; Vékely, K. *MassKinetics* www.chemres.hu/ms/masskinetics 2001.

(42) Drahos, L.; Vékely, K. *J. Mass Spectrom.* **2001**, *36*, 237–263.

(43) Paizs, B.; Suhai, S. *Mass Spectrom. Rev.* **2005**, *24*, 508–548.

(44) Schmier, P. D.; Price, W. D.; Strittmatter, E. F.; Williams, E. R. *J. Am. Soc. Mass Spectrom.* **1997**, *8*, 771–780.

exponential factors, would yield better agreement between experimental and theoretical spectra, but this was not attempted.

RESULTS AND DISCUSSION

Leucine Enkephalin: Relative Energy of Fragment Ion Formation. Leucine enkephalin contains five amino acids with the sequence tyrosine-glycine-glycine-phenylalanine-leucine (YGGFL). In general, protonated peptides tend to cleave at the amide bonds along the peptide backbone when CID is used as the ion activation method. Assuming a singly protonated peptide, if the charge remains on the N-terminal side of the peptide, the product ion is termed b_n , where n refers to the number of amino acid residues counting from the N-terminus. Likewise, if the charge remains on the C-terminal side of the peptide, the fragment is identified as a y_n ion, where n is determined by counting amino acid residues from the C-terminus.⁴⁵ The formation of a_n ions commonly occurs via a loss of CO from b_n ions.^{46–49}

In the case of leucine enkephalin, the lowest energy fragmentation process is formation of b_4 ; this is typically the most abundant fragment in the case of SORI-CID and BIRD studies⁴⁴ ($m/z = 425.2$, Figure 1a). Medium-energy fragments include the a_4 ion ($m/z = 397.2$, Figure 1a), which can be formed by the loss of CO from b_4 . The a_4/b_4 ratio is sometimes used to characterize the degree of excitation.^{50,51} Other medium-energy fragments are the b_3 ($m/z = 278.1$) and y_2 ($m/z = 279.2$) ions. Alexander and Boyd⁵² first suggested the use of the b_3/y_2 ratio as a sensitive measure for internal energy deposition into the precursor ions, and this ratio has been used elsewhere.⁵¹ The b_3 ion results from a higher energy fragmentation pathway; therefore, an increasing b_3/y_2 ratio indicates increasing energy content in the molecule.

Formation of immonium ions is characteristic of high-energy processes (i.e., greater energy requirements than any of the ions, b_4 , a_4 , b_3 , and y_2 , considered here), and these immonium ions are only rarely observed with high abundance in FT-ICR CID.^{53–59} In the case of leucine enkephalin, immonium ions derived from phenylalanine (F) ($m/z = 120.1$) and tyrosine (Y) ($m/z = 136.1$) are expected. These immonium ions are indeed observed in SORI-RE (Figure 1c), while they are of very low abundance in the SORI-CID spectrum (Figure 1a). The abundance of $a_4 + b_4$

ions compared to that of the Y + F ions is a good measure of the degree of excitation in leucine enkephalin; e.g., SID and keV CID spectra contain abundant immonium ions.⁴⁵

Leucine Enkephalin: Comparison of SORI-CID, RE-CID, SORI-RE-CID, and RE-SORI-CID Spectra. Figure 1a–c shows respectively the spectra obtained experimentally by SORI, RE, and SORI-RE CID fragmentation of the monoisotopically selected YGGFL(H^+) ion using argon as the collision gas. When the YGGFL(H^+) ion is fragmented via a 2.0-V, 500-ms SORI pulse (Figure 1a), the a_4 and b_4 ions are the most abundant fragment ions and these ions are present at an a_4/b_4 ratio of ~ 0.3 . By contrast, when a 120-V, 10- μ s RE pulse is applied (Figure 1b), the a_4 ion becomes more abundant than the b_4 ion. Also, the F and Y immonium ions, which result from higher energy fragmentation processes, are barely detectable in the SORI spectrum but are observable as ions of low abundance in RE. The b_3 and y_2 ions are present at a similar ratio in both the SORI and RE spectra.

The enhancement of higher energy fragmentation processes occurs when the 120-V, 10- μ s RE pulse is applied 20 ms after the completion of the 2.0-V, 500-ms SORI pulse (Figure 1c). First, the a_4 and b_4 ions, while still very abundant, are not the only main fragment ions present. The F and Y immonium ions are much more abundant in the SORI-RE spectrum than in either the SORI or the RE spectra. The b_3 and y_2 ions are also enhanced as compared to SORI and RE alone. In contrast to the SORI and RE spectra, the SORI-RE spectrum has a y_2 ion less intense than the b_3 ion, also indicating a change in energy deposition. In addition, the singly charged ion at m/z 323 is enhanced compared to either SORI or RE. In the previously reported multistep mechanism for the formation of the m/z 323 ion, the a_4 ion loses NH_3 and undergoes a cyclic rearrangement. The rearranged ion has a previous internal residue (glycine) at the new N-terminus, and this glycine residue is readily lost, forming the ion at m/z 323.⁶⁰ Therefore, it appears that combining SORI with RE has a synergistic effect; i.e., SORI-RE is not a simple linear combination of SORI and RE. Fragment ions resulting from higher energy channels are enhanced as compared to RE alone. In addition, the abundance of low-energy fragment ions common in SORI spectra is maintained. A further advantage of SORI-RE is that it is easy to optimize and to perform.

Changing the sequence of ion activation and performing RE first followed by a SORI cycle is also possible, but in such a case, the results depend significantly on the time gap between the RE and SORI pulses. Figure 2c,d shows the RE-SORI spectra when the gap between RE and SORI pulses is 20 and 50 ms, respectively, along with the corresponding SORI and RE spectra for comparison (Figure 2a,b). The collision gas valve was opened 500 ms before the RE pulse and closed at the end of the SORI pulse, resulting in an overall pulse time of 1020–1050 ms, depending on the time gap (compared to 550 ms for SORI-RE). This is necessary during RE-SORI due to the short duration of the RE pulse. Therefore, the precursor ion is depleted to a greater extent in the SORI and RE spectra shown in Figure 2a,b than in Figure 1a,b due to the higher collision gas pressure in the ICR cell. As expected, the highest abundance SORI fragment ions observed (i.e., a_4 , b_4) with a 2.0-V, 500-ms pulse are those resulting from lower energy

(45) Biemann, K. *Biomed. Environ. Mass Spectrom.* **1988**, *16*, 99–111.

(46) Farrugia, J. M.; O'Hair, R. A. J.; Reid, G. E. *Int. J. Mass Spectrom.* **2001**, *210*, 71–87.

(47) Ambihapathy, K.; Yalcin, T.; Leung, H. W.; Harrison, A. G. *J. Mass Spectrom.* **1997**, *32*, 209–215.

(48) Yalcin, T.; Csizmadia, I. G.; Peterson, M. R.; Harrison, A. G. *J. Am. Soc. Mass Spectrom.* **1996**, *7*, 233–242.

(49) Yalcin, T.; Khouw, C.; Csizmadia, I. G.; Peterson, M. R.; Harrison, A. G. *J. Am. Soc. Mass Spectrom.* **1995**, *6*, 1165–1174.

(50) Thibault, P.; Alexander, A. J.; Boyd, R. K.; Tomer, K. B. *J. Am. Soc. Mass Spectrom.* **1993**, *4*, 845–854.

(51) Vachet, R. W.; Glish, G. L. *J. Am. Soc. Mass Spectrom.* **1996**, *7*, 1194–1202.

(52) Alexander, A. J.; Boyd, R. K. *Int. J. Mass Spectrom. Ion Processes* **1989**, *90*, 211–240.

(53) Falick, A. M.; Hines, W. M.; Medzihradzky, K. F.; Baldwin, M. A.; Gibson, B. W. *J. Am. Soc. Mass Spectrom.* **1993**, *4*, 882–893.

(54) Biemann, K. *Methods Enzymol.* **1990**, *193*, 455–479.

(55) Madden, T.; Welham, K. J.; Baldwin, M. A. *Org. Mass Spectrom.* **1991**, *26*, 443–446.

(56) Johnson, R. S.; Biemann, K. *Biomed. Environ. Mass Spectrom.* **1989**, *18*, 945–957.

(57) Biemann, K.; Scoble, H. A. *Science* **1987**, *237*, 992–998.

(58) Biemann, K.; Martin, S. A. *Mass Spectrom. Rev.* **1987**, *6*, 1–75.

(59) Lippstreufisher, D. L.; Gross, M. L. *Anal. Chem.* **1985**, *57*, 1174–1180.

(60) Vachet, R. W.; Bishop, B. M.; Erickson, B. W.; Glish, G. L. *J. Am. Chem. Soc.* **1997**, *119*, 5481–5488.

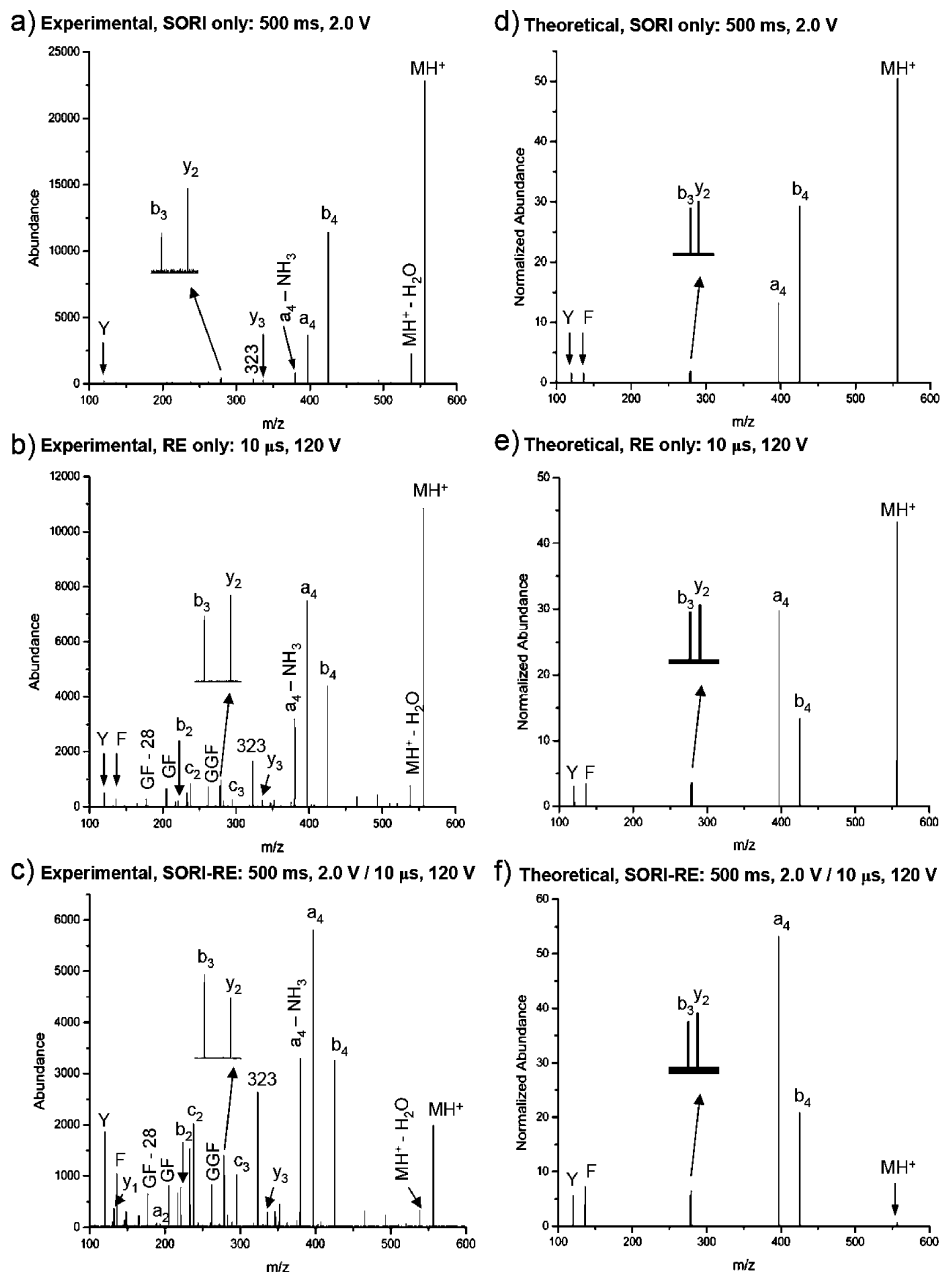


Figure 1. Experimental and calculated fragmentation spectra for the monoisotopically selected YGGFL(H^+) ion using argon as the collision gas (550 ms pulse). (a) Experimental SORI: time 500 ms, amplitude 2.0 V. (b) Experimental RE: time 10 μ s, amplitude 120 V. (c) Experimental SORI-RE: SORI time 500 ms, amplitude 2.0 V, 20-ms time gap, RE time 10 μ s, amplitude 120 V. (d) Theoretical SORI: time 500 ms, amplitude 2.0 V. (e) Theoretical RE: time 10 μ s, amplitude 120 V. (f) Theoretical SORI-RE: SORI time 500 ms, amplitude 2.0 V, 20-ms time gap, RE time 10 μ s, amplitude 120 V.

fragmentation processes (Figure 2a). In addition, the b_3/y_2 and a_4/b_4 ion ratios are both ~ 0.2 . Figure 2b shows the result of a 10- μ s, 120-V RE pulse. In this spectrum, a_4 and b_4 remain the highest abundance fragment ions. However, the F immonium, b_3 , and y_2 ions are present at a higher abundance than in the SORI spectrum. The Y immonium ion, barely detected in the SORI spectrum, is of higher abundance with RE. In addition, the b_3/y_2 and a_4/b_4 ion ratios have increased to 0.4 and 2.3. Figure 2c,d shows the result of combining the SORI and RE pulses from Figure 2a,b, with RE preceding SORI. In Figure 2c, there is a 20-ms gap between the activation pulses, the shortest time gap allowed by the hardware. In this spectrum, the F immonium, Y immonium, m/z 323, b_3 , and y_2 ions are enhanced as compared

to SORI or RE alone. The b_3/y_2 and a_4/b_4 ion ratios are 1.1 and 2.7, respectively, indicating a higher level of energy deposition. By contrast, the RE-SORI spectrum shown in Figure 2d with a 50-ms gap between activation pulses looks more similar to Figure 2b. First, the F immonium, Y immonium, m/z 323, b_3 , and y_2 ion abundances are very similar to the RE spectrum in Figure 2b and less than the RE-SORI spectrum in Figure 2c (20-ms gap). Second, the b_3/y_2 and a_4/b_4 ion ratios are 0.7 and 2.4. While these ratios are somewhat higher than the ion ratios for RE alone, they are significantly smaller than the RE-SORI spectrum with a 20-ms gap between activation pulses. The spectral differences shown in Figure 2c and d illustrate that the precursor ions undergo collisional cooling when the gap between the RE and SORI pulses

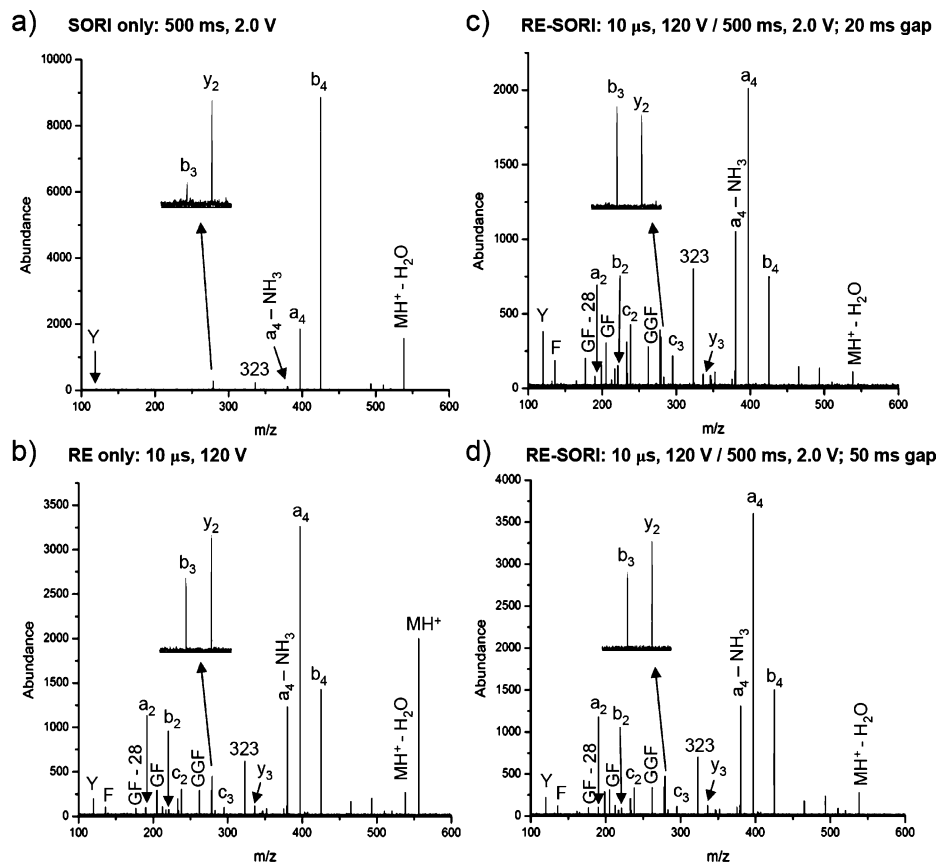


Figure 2. Experimental fragmentation spectra for the monoisotopically selected YGGFL(H⁺) ion using argon as the collision gas (1050 ms pulse). (a) SORI: time 500 ms, amplitude 2.0 V. (b) RE: time 10 μs, amplitude 120 V. (c) RE-SORI: RE time 10 μs, amplitude 120 V, 20-ms time gap, SORI time 500 ms, amplitude 2.0 V. (d) RE-SORI: RE time 10 μs, amplitude 120 V, 50 ms time gap, SORI time 500 ms, amplitude 2.0 V.

is 50 ms or greater. Also, when the gap between the RE and SORI pulses is short (i.e., 20 ms), more precursor ions may remain off-axis than with a longer time gap. It is important to note that the timing between the SORI and RE pulses when SORI is performed first is also important, although not as critical. If RE is performed 200 ms or less after SORI (data not shown), the spectrum is similar to that shown in Figure 1c. One advantage to performing SORI before RE is the lesser amount of collision gas that needs to be pumped away before detection. If RE is performed before SORI, the gas must be pulsed in several hundred milliseconds before the RE pulse. Also, when RE is performed first, off-axis ions lead to a radial loss of product ions, as well as precursor ions for the subsequent SORI stage.

SORI, RE, and SORI-RE spectra of YGGFL(H⁺) were also studied by theoretical modeling using MassKinetics.⁴² The three spectra were calculated as described in the Experimental Section using only five adjustable parameters, most of these to account for the unknown activation energies of several fragmentation processes. The main spectral features of the calculated spectra (Figure 1d–f) correspond closely to those experimentally observed (Figure 1a–c): the a₄/b₄ ratio characterizes the medium-high excitation energy range, showing increasing excitation in the order of SORI, RE, and SORI-RE. The a₄ and b₄ ion abundances follow the same trend in the experimental and theoretical spectra. The abundance of Y and F ions is characteristic of a high degree of excitation by SORI-RE, and the experimental and theoretical spectra show reasonable agreement. The medium-energy y₃ and

b₂ ions are of low abundance in both the observed and calculated spectra. The modeling results are quite promising, showing that the experimental and theoretical spectra follow the same trend, and the observed results are in reasonable agreement with theoretical expectations, even using only a few adjustable parameters. The theoretical results confirm that differences among SORI, RE, and SORI-RE spectra are due to internal energy variations using the three different excitation methods.

Differences in the spectra of SORI, RE, and SORI-RE are relatively easy to explain using internal energy distributions. The average internal energy distribution changes with time. This time dependence is due to an increase in the average internal energy during excitation and a decrease when excitation stops because of fragmentation and collisional and radiative cooling. Figure 3 shows the internal energy distributions at the time when the average internal energy is at its maximum value (i.e., immediately following the excitation period). These internal energy distributions were calculated using experimental conditions as specified for Figure 1. The collisions in RE are higher in kinetic energy as compared to SORI. However, the number of collisions is much smaller in RE. This results in a slightly higher mean internal energy in SORI than in RE, although RE is capable of producing high internal energy ions (but in low abundance only). This explains the higher abundance of the a₄ ion (note especially the a₄/b₄ ratio, as discussed in detail below) and the increased abundance of the medium- (b₃, y₂) and the high-energy ions (Y and F). Note also that the internal energy distribution increases

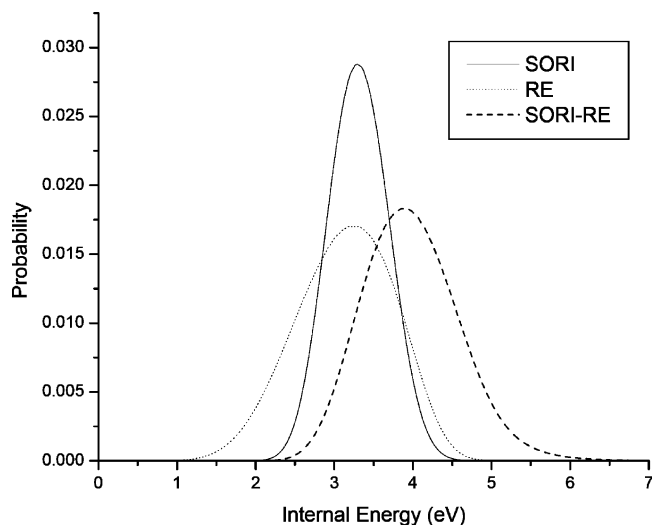


Figure 3. Calculated internal energy distribution of YGGFL(H⁺) using experimental conditions as specified in Figure 1 for SORI (corresponding to 90% parent ion decomposition), RE (at maximum average internal energy, see text), and SORI-RE (at maximum average internal energy, see text).

only slightly if SORI is performed for a long time (as may be expected from a “slow heating” technique, data not shown). Figure 3 illustrates of why SORI-RE is capable of producing abundant high-energy fragments: the tail of the internal energy distribution extends far higher than would be obtainable by SORI only, and the average internal energy deposited by SORI-RE is also higher.

Leucine Enkephalin: Effect of SORI and RE Time and Amplitude on the Relative Abundances of the a_4 , b_4 , F, Y, and MH⁺ Ions. Systematic measurements have been performed to study the effect of SORI and RE excitation time and voltages. Figure 4 shows the experimental and theoretical relative ion abundances of the precursor ion, two lower-energy fragment ions ($a_4 + b_4$), and two higher-energy fragment ions (F + Y) when SORI is used in conjunction with argon as the collision gas to fragment the monoisotopically selected YGGFL(H⁺) precursor ion. When SORI amplitude is held constant at 2.0 V and time is varied from 50 to 2000 ms (Figure 4a), the precursor ion is almost completely depleted after 700 ms. The ($a_4 + b_4$) abundance levels off at ~75% of the total ion abundance after 700 ms. The (F + Y) abundance is insignificant and never rises above 1.3% of the total ion abundance. These results indicate that even though MH⁺ fragments completely, most of the fragmentation of the parent ion is occurring through low-energy channels leading to the formation of the a_4 and b_4 ions. In Figure 4b, SORI time is held constant at 500 ms while SORI amplitude is varied from 0 to 4.0 V. Similar to the case in which SORI voltage is kept constant, the a_4 and b_4 ions are the most significant. However, increasing the SORI amplitude beyond 2.5 V results in a decline of the ($a_4 + b_4$) relative abundance as other fragment ions (i.e., $b_4 - \text{NH}_3$, b_3 , y_2) gain in prominence. Also, the (F + Y) relative ion abundance is not insignificant in this case, but rather begins to increase after 3.0 V and reaches ~7% of the total ion abundance by 4.0 V. Therefore, as SORI amplitude is increased, more energy is deposited into the precursor ion leading to higher energy fragment ions. However, this is not extremely useful for the detection of higher energy fragment ions in this case because signal is rapidly

lost as amplitude is increased beyond 4.0 V, presumably due to excitation of the precursor ion beyond the dimensions of the ICR cell.

The dependence of SORI spectra on excitation time and on excitation amplitude has also been studied by theoretical (Mass-Kinetics) modeling. Using the same parameters used to calculate the spectra shown in Figure 1d,e, time- and excitation amplitude-dependent ion ratios were also calculated, and the results are shown in Figure 4c,d. The survival yield of the precursor ion and the relative abundances of the a_4 and b_4 ions are good indications for increasing internal energy content, and these are in satisfactory agreement with the curves obtained experimentally (Figure 4a,b). The abundance of the high-energy Y and F ions is somewhat higher in the calculated spectra than that observed experimentally, but the trend with increasing SORI time and increasing SORI amplitude is similar. This suggests that there is a general agreement of trends but not in absolute values of ion abundances between experimental and theoretical spectra. The “saturation-type” curve suggests that SORI itself is not capable of producing high-energy ions in large abundance even if done for a long time or at a higher amplitude.

Systematic measurements have also been performed to examine the effect of RE amplitude and time. Figure 5a shows the relative abundances of the parent, ($a_4 + b_4$), and (F + Y) ions when RE amplitude is kept constant at 85 V and RE excitation time is varied from 10 to 15 μs . The precursor ion’s signal steadily decreases and is <7% of the total ion abundance by 15 μs . The relative abundance of the ($a_4 + b_4$) ions reaches a maximum of ~40% around 12 μs and is less dominant than in the SORI spectra. By 15 μs , the abundance of the (F + Y) ions has risen to ~5% of the total ion abundance but is not much more significant than in the SORI ion abundance curves (Figure 4a,b).

In Figure 5b, RE time is held constant at 10 μs while RE amplitude is increased from 50 to 150 V. Spectral appearance is quite similar to the case in which RE amplitude is held constant and time varied. The precursor ion signal steadily decreases and is <3% of the total ion abundance at 150 V. The (F + Y) immonium ions reach a relative abundance of ~9% at 150 V. Also, the abundance of the ($a_4 + b_4$) ions first increases, reaches a maximum of ~40% at 115 V, and then declines to <16% by 150 V. It is likely that 10- μs RE pulses below 115 V are not energetic enough to allow the parent ion to extensively access higher energy fragmentation pathways, and so activation results mainly in the a_4 and b_4 ions. At 100 V, the parent ion relative abundance is still 50%. Beyond 115 V, higher fragmentation channels are accessible and the a_4 and b_4 ions decline in relative abundance as higher energy fragment ions become more dominant.

Leucine Enkephalin: Effect of SORI and RE Time and Amplitude on the Ratios of the a_4/b_4 and b_3/y_2 Ions. Figure 6 shows the ratios of a_4/b_4 and b_3/y_2 ions for SORI and RE activation. As mentioned earlier, a_4 and b_3 ions are considered as resulting from higher energy fragmentation channels than b_4 and y_2 ions, respectively. A ratio greater than 1 is therefore an indication of the fragment ion resulting from the higher energy channel occurring more frequently than the corresponding lower energy fragment ion. One notable feature of these plots is that, for the case in which SORI voltage is held constant at 2.0 V and SORI time varied (Figure 6a), both a_4/b_4 and b_3/y_2 ratios are small,

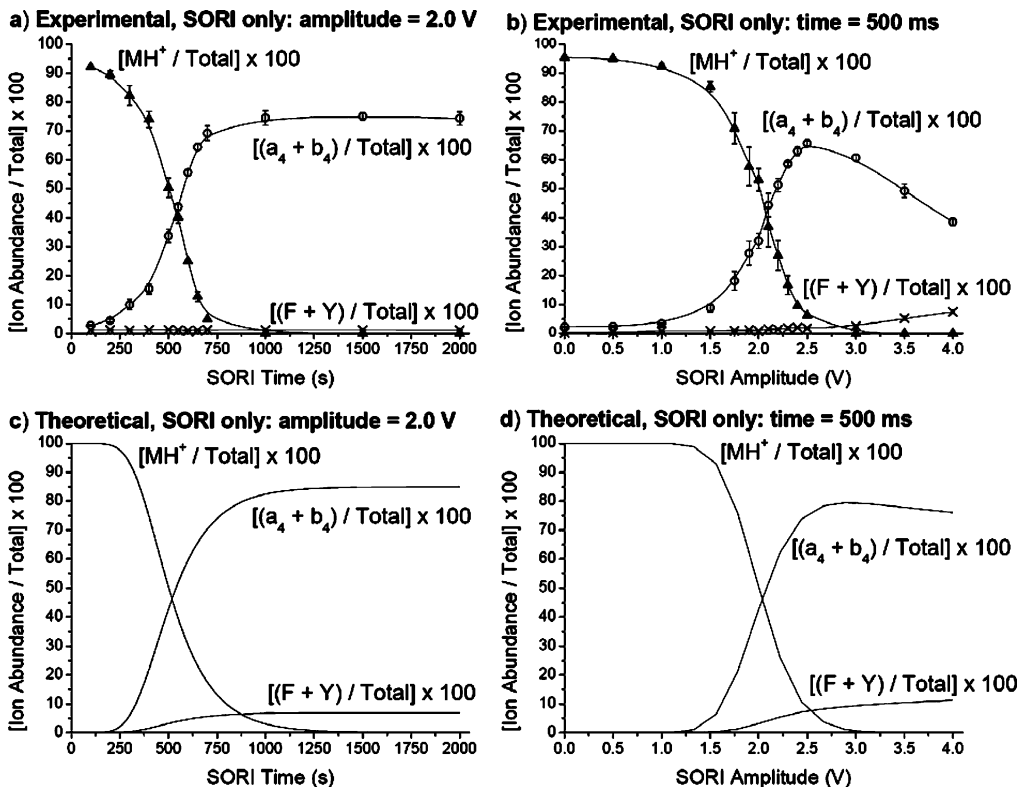


Figure 4. Experimental and theoretical relative ion abundances of the $(a_4 + b_4)$, $(F + Y)$ immonium, and MH^+ ions resulting from the monoisotopic selection and fragmentation of $YGGFL(H^+)$ using argon as the collision gas. (a) Experimental, SORI amplitude 2.0 V, vary time. (b) Experimental, SORI time 500 ms, vary amplitude. (c) Theoretical, SORI amplitude 2.0 V, vary time. (d) Theoretical, SORI time 500 ms, vary amplitude.

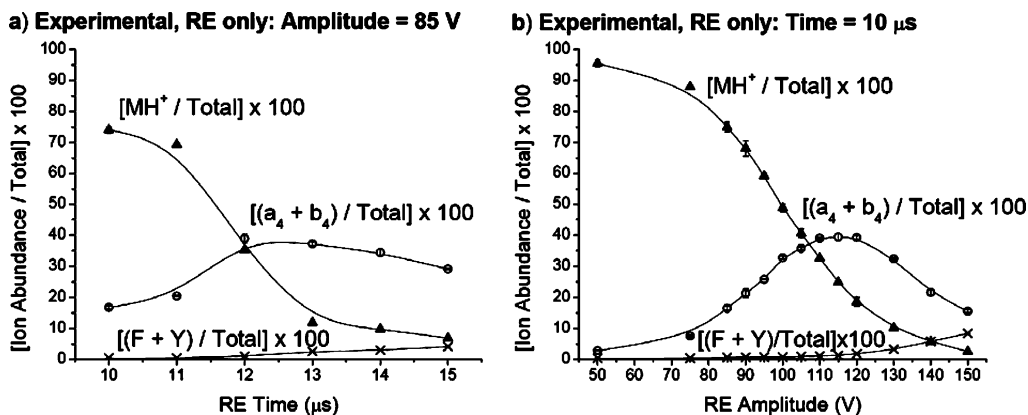


Figure 5. Experimental relative ion abundances of the $(a_4 + b_4)$, $(F + Y)$ immonium, and MH^+ ions resulting from the monoisotopic selection and fragmentation of $YGGFL(H^+)$ using argon as the collision gas/ (a) RE amplitude 85 V, vary time. (b) RE time 10 μs , vary amplitude.

indicating low excitation. Therefore, increasing SORI time does not deposit greater amounts of internal energy but rather leads to the lower energy fragment ions because energy deposition occurs in small, sequential steps. In a manner similar to holding SORI amplitude constant, when SORI duration is held constant at 500 ms and amplitude varied from 0 to 4.0 V (Figure 6b), both ratios initially remain below 1 and increase as a function of amplitude. By 4.0 V, the a_4/b_4 ratio reaches 3.2 and the b_3/y_2 ratio reaches 0.5. Increasing SORI amplitude high enough to observe intense fragment ions resulting from higher energy pathways leads to the rapid loss of signal due to excitation of the precursor ion beyond the dimensions of the ICR cell.

Figure 6c,d shows the effect of on-resonant excitation of $YGGFL(H^+)$ on the a_4/b_4 and b_3/y_2 ratios. Whereas both ratios were, in general, below 1 for SORI activation, they are more often above 1 for RE. When RE amplitude is held constant at 85 V and time varied from 10 to 15 μs (Figure 6c), the a_4/b_4 and b_3/y_2 ratios are greater than 1 by 12 and 15 μs , respectively. When RE duration is held constant at 10 μs and amplitude increased from 50 to 150 V (Figure 6d), the a_4/b_4 ratio initially decreases slightly, but then steadily increases and reaches 3.6 at 150 V. The b_3/y_2 ratio reaches 1.8 at 150 V. These data demonstrate that, if excitation time and amplitude are large enough, RE alone is able to deposit larger amounts of energy at once than SORI alone, causing higher abundances of fragment ions that result from higher energy fragmentation channels. However, attempts to increase the abundance of higher energy fragment ions by increasing the

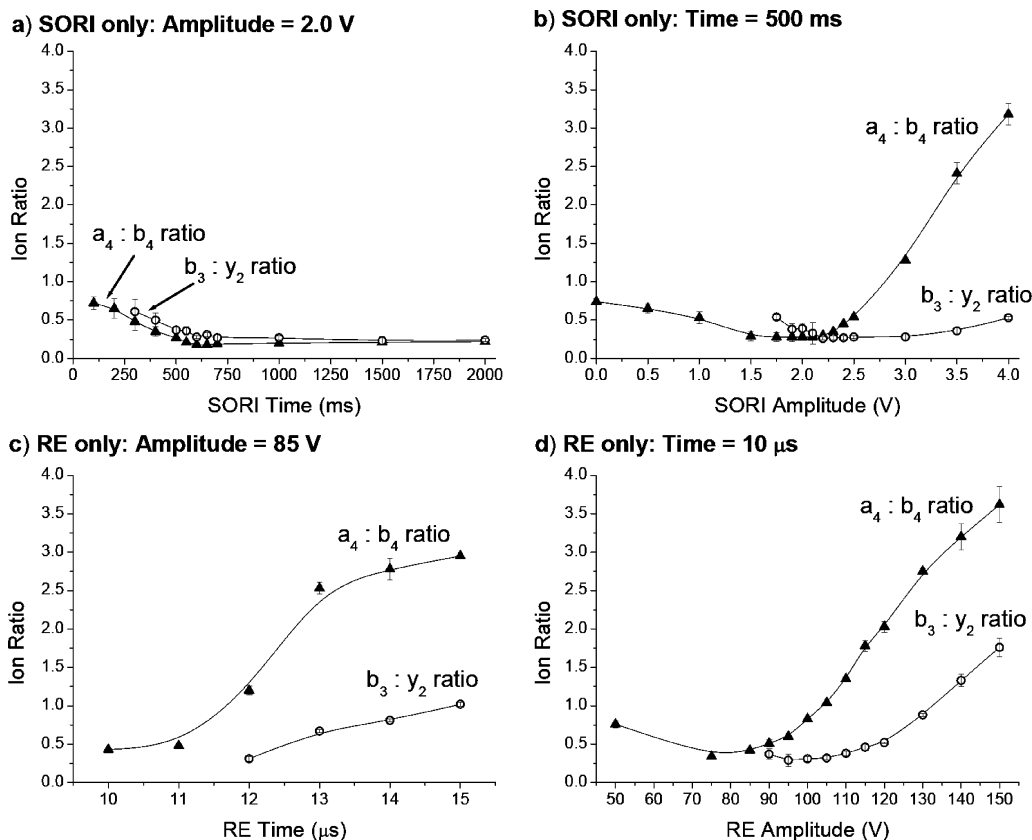


Figure 6. Experimental ratios of a_4/b_4 and b_3/y_2 ions resulting from the monoisotopic selection and fragmentation of YGGFL(H^+) using argon as the collision gas. (a) SORI amplitude 2.0 V, vary time. (b) SORI time 500 ms, vary amplitude. (c) RE amplitude 85 V, vary time. (d) RE time 10 μ s, vary amplitude.

RE amplitude and time also leads to a rapid loss of signal intensity.

2 α -Mannobiose and 3 α -Mannobiose: Comparison of SORI, RE, and SORI-RE CID Spectra. Common fragment ions resulting from the CID of oligosaccharides include cleavage at the glycosidic linkage and cross-ring cleavages. Cleavage at glycosidic linkages, in general, results from lower energy fragmentation pathways. The SORI, RE, and SORI-RE CID spectra for two simple lithium-cationized disaccharides differing only in the position of the glycosidic linkage, 2 α -mannobiose and 3 α -mannobiose, are shown in Figure 7. The SID spectra of these disaccharides, along with 4 α - and 6 α -mannobiose, have been previously reported.⁶¹ In this study, Dongré and Wysocki used the presence of specific cross-ring product ions to characterize the position of the glycosidic linkage.

As shown in Figure 7, two fragment ions result from the cleavage of the glycosidic linkage, labeled Z_1^+ (m/z 169.1) and Y_1^+ (187.1). The Y_1^+ ion contains one of the hexose rings with the glycosidic linkage oxygen plus a hydrogen, while the Z_1^+ ion corresponds to the Y_1^+ ion by a formal loss of H_2O . The 500-ms, 1.8-V SORI-CID spectrum of 2 α -mannobiose is shown in Figure 7a. The most abundant fragment ions are Y_1^+ , Z_1^+ , and m/z 229.1. The ion at m/z 229.1 is the result of a cross-ring cleavage and corresponds to a loss of $C_4H_8O_4$ from the precursor ion. This ion was used previously in the SID spectrum to characterize the position of the glycosidic linkage.⁶¹ Three additional ions at m/z

97.0 ($LiC_3H_6O_3^+$), 127.1 ($LiC_4H_8O_4^+$), and 259.1 (loss of $C_3H_6O_3$ from precursor ion) also result from cross-ring cleavages and are present at low abundances. In Figure 7b, 2 α -mannobiose is fragmented via a 10- μ s, 105-V RE pulse. The Y_1^+ and Z_1^+ ions remain the most abundant. The cross-ring cleavage ion at m/z 127.1, which was of very low abundance in the SORI spectrum, is now more abundant than the cross-ring cleavage ion at m/z 229.1. A cross-ring cleavage ion at m/z 91.0 ($LiC_4H_4O_2^+$), absent in the SORI spectrum, is observed in the RE spectrum. Also, the abundance of the cross-ring cleavage ion at m/z 259.1 in the RE spectrum is very low and similar to the SORI spectrum. Figure 7c shows the result of applying the 10- μ s, 105-V RE pulse 20 ms after the 500-ms, 1.8-V SORI pulse. In this spectrum, the cross-ring cleavage ion at m/z 127.1 is now almost as abundant as the Z_1^+ ion. Cross-ring cleavage ions at m/z 91.0 and 97.0 are also enhanced. As in the SORI and RE spectra, the cross-ring cleavage ion at m/z 259.1 remains of low abundance relative to the other fragment ions discussed.

The SORI, RE, and SORI-RE CID for 3 α -mannobiose results in the observation of the same fragment ions as for 2 α -mannobiose, but in different relative abundances. In Figure 7d, the 500-ms, 1.5-V SORI spectrum is shown for 3 α -mannobiose with argon as the collision gas. As expected, the glycosidic linkage cleavage ions, Y_1^+ and Z_1^+ , are two of the most abundant fragment ions. However, unlike the SORI spectrum for 2 α -mannobiose, the loss of H_2O from the precursor ion is the most abundant fragment ion in the spectrum. Also, the Z_1^+ ion is more abundant than the Y_1^+

(61) Dongré, A. R.; Wysocki, V. H. *Org. Mass Spectrom.* **1994**, *29*, 700–702.

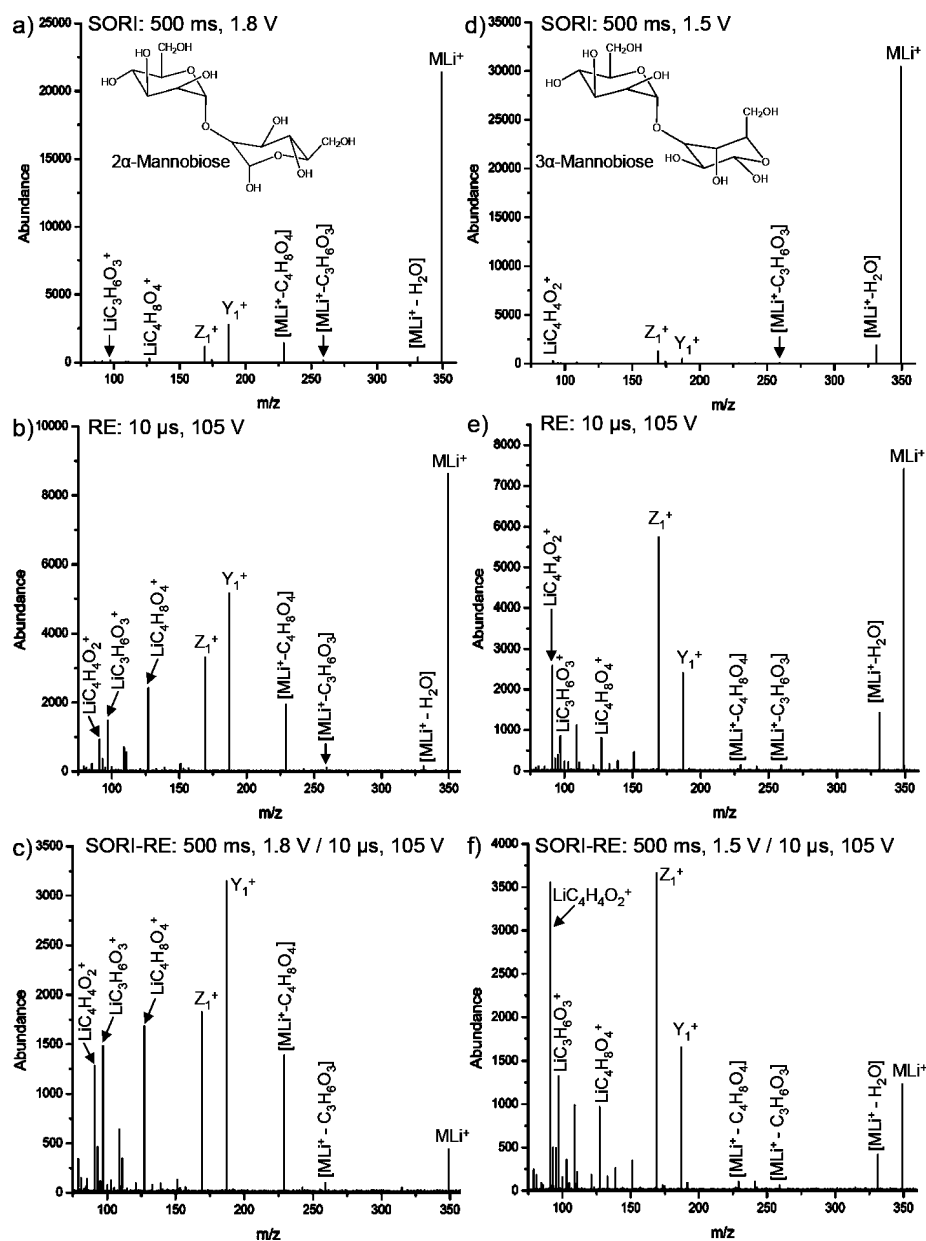


Figure 7. Experimental fragmentation spectra of the monoisotopically selected lithium-cationized 2 α -mannobiose and 3 α -mannobiose ions using argon as the collision gas (550-ms pulse). (a) 2 α -mannobiose, SORI: time 500 ms, amplitude 1.8 V. (b) 2 α -mannobiose, RE: time 10 μ s, amplitude 105 V. (c) 2 α -mannobiose, SORI-RE: SORI time 500 ms, amplitude 1.8 V, 20-ms time gap, RE time 10 μ s, amplitude 105 V. (d) 3 α -mannobiose, SORI: time 500 ms, amplitude 1.5 V. (e) 3 α -mannobiose, RE: time 10 μ s, amplitude 105 V. (f) 3 α -mannobiose, SORI-RE: SORI time 500 ms, amplitude 1.5 V, 20-ms time gap, RE time 10 μ s, amplitude 105 V.

ion. The cross-ring cleavage ions at m/z 91.0 and 259.1 are present at very low abundances, while the cross-ring cleavage ions at m/z 97.0, 127.1, and 229.1 are absent. Figure 7e shows the 10- μ s, 105-V RE spectrum of 3 α -mannobiose. While the Z_1^+ ion remains the most abundant fragment ion, the cross-ring cleavage ion at m/z 91.0 is more abundant than the Y_1^+ ion. The cross-ring cleavage ions at m/z 97.0, 127.0, and 229.1, absent in the SORI spectrum, are clearly observed. The 500-ms, 1.5-V/10- μ s, 105-V SORI-RE CID spectrum of 3 α -mannobiose is shown in Figure 7f. The cross-ring cleavage ion at m/z 91.0 is now almost as abundant as the Z_1^+ ion and significantly more abundant than the Y_1^+ ion. The relative abundances of the cross-ring cleavage ions at m/z 91.0, 97.0, and 127.1 follow the trend: m/z 91.0 > 97.0 > 127.1. However, in the 2 α -mannobiose SORI-RE spectrum, this trend is

reversed with the relative abundances in the order m/z 127.1 > 97.0 > 91.0. Also, the relative abundance of the cross-ring cleavage ions at m/z 229.1 and 259.1 is low and shows no significant change in Figure 7f as compared to the RE spectrum in Figure 7e.

The comparison of the SORI, RE, and SORI-RE spectra for 2 α -mannobiose and 3 α -mannobiose demonstrates that the relative abundances of the glycosidic linkage and cross-ring cleavage ions change as the internal energy of the precursor ion is increased. In particular, some cross-ring cleavage ions become enhanced as compared to cleavage at the glycosidic linkage. However, the abundances of other cross-ring cleavage ions remain relatively unchanged. As also demonstrated for 2 α -mannobiose and 3 α -mannobiose, the location of the glycosidic linkage effects the relative abundances of different fragment ions observed, and these

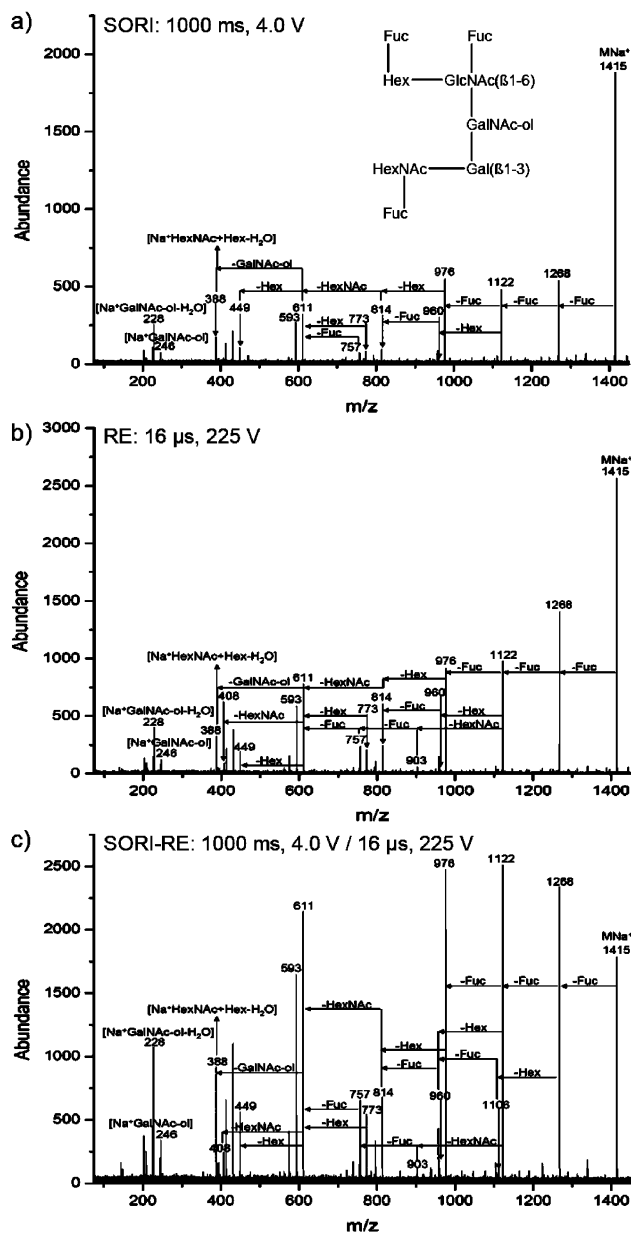


Figure 8. Fragmentation of the monoisotopically selected Alditol XT + Na⁺ ion using nitrogen as the collision gas. (a) SORI: time 1000 ms, amplitude 4.0 V. (b) RE: time 16 μs, amplitude 225 V. (c) SORI-RE: SORI time 1000 ms, amplitude 4.0 V, 20-ms time gap, RE time 16 μs, amplitude 225 V.

ion abundances show different amounts of enhancement as the internal energy of the precursor ion is increased. These differences may lead to insights into fragmentation mechanisms and relative energy requirements for fragmentation pathways.

Alditol XT: Comparison of SORI, RE, and SORI-RE CID Spectra. SORI, RE, and SORI-RE CID are demonstrated in Figure 8 for the sodiated ions of an oligosaccharide, alditol XT. The SORI-CID (MS² and MS⁵, *m/z* 1415/1268.5/1122.4/976.3) and IRMPD spectra of this sodiated oligosaccharide have been previously reported by Lebrilla and co-workers.⁵ In their study, IRMPD was capable of producing low relative abundance lower mass fragment ions (i.e., *m/z* 228.1, 388.1, 408.1, 449.1, identified in Figure 8) that were observed with a slightly higher relative abundance but with a lower overall signal intensity during MS⁵.

The authors also reported that these fragment ions are observed using energetic SORI conditions during MS² but that signal intensity and the abundance of the higher mass fragment ions are depleted. The loss of one, two, and three fucose units from the sodiated alditol XT (MNa⁺) ion results in fragment masses of *m/z* 1268.5, 1122.4, and 976.3, respectively. These are the most abundant fragment ions observed in the SORI, RE, and SORI-RE spectra shown in Figure 8. Other fragment ions resulting from the cleavage of multiple glycosidic linkages are identified in Figure 8. Figure 8a shows the 1000-ms, 4.0-V SORI spectrum with nitrogen as the collision gas. In this spectrum, the fragment ions resulting from the loss of one to three fucose rings are present at less than 30% relative abundance, while all other fragment ions are 20% relative abundance or less. In the 16-μs, 225-V RE spectrum shown in Figure 8b, the ions corresponding to the loss of one to three fucose rings are less than 50% relative abundance while all other fragment ions are less than 30% relative abundance. However, when the SORI and RE pulses are combined, as shown in Figure 8c, many fragment ions are present at a relative abundance of greater than 50% and the overall extent of fragmentation is much greater as compared to Figure 8a,b. It is important to note that the extent of fragmentation observed in the SORI-RE spectrum shown in Figure 8c is not achieved, due to a loss of signal, when SORI or RE alone is used even with a longer or a higher amplitude pulse. In addition, the extent of fragmentation observed with the SORI-RE technique is much greater than that reported by Lebrilla and co-workers for either SORI-CID (MS² and MS⁵) or IRMPD.⁵ In this alditol XT example, SORI-RE provides an improvement in fragmentation efficiency and signal-to-noise ratio over SORI and RE alone, as well as the reported SORI-CID MS² and MS⁵, and IRMPD spectra.⁵

SORI, RE, and SORI-RE CID Fragmentation of [Ubiquitin + 10H]¹⁰⁺. Figure 9a–c shows the SORI, RE, and SORI-RE CID fragmentation spectra of ubiquitin with 10 protons. Argon was used as the collision gas in these experiments. These spectra show some similarities to those obtained by BIRD by Williams and co-workers.⁶² By comparison of the SORI and SORI-RE spectra in Figure 9a,c, it is seen that the *y*₁₈³⁺, *y*₁₈²⁺, and *y*₁₂²⁺ ions are more abundant in the SORI-RE spectrum than in the SORI spectrum. This indicates that the amide bond cleavage between the amino acids Asp⁵⁸-Tyr⁵⁹ (*y*₁₈ⁿ⁺) and Glu⁶⁴-Ser⁶⁵ (*y*₁₂²⁺) is more efficient when a RE pulse is applied after the SORI excitation. Furthermore, the ratio of *y*₁₈³⁺/*y*₂₄⁴⁺ ions is greater than 1 in the SORI-RE spectrum but less than 1 in the SORI and RE spectra. This result indicates that the amide bond cleavage at Asp⁵⁸-Tyr⁵⁹ (*y*₁₈ⁿ⁺) increases relative to Asp⁵²-Gly⁵³ (*y*₂₄⁴⁺) at higher internal energies. We also note that the abundances of several ions in the *m/z* 1100–1400 region increase with increasing internal energy (i.e., in the SORI-RE spectrum relative to the SORI spectrum). Although the differences among the SORI, RE, and SORI-RE spectra do not allow us to directly derive mechanistic information, this information does provide insight into relative energy requirements for specific bond cleavages (i.e., *y*₁₈ formation appears to have greater energy requirements than *y*₂₄ formation).

SORI, RE, and SORI-RE CID Fragmentation of the Singly Charged Uranyl Cation (UO₂⁺). Finally, we show another

(62) Jockusch, R. A.; Schnier, P. D.; Price, W. D.; Strittmatter, E. F.; Demirev, P. A.; Williams, E. R. *Anal. Chem.* **1997**, *69*, 1119–1126.

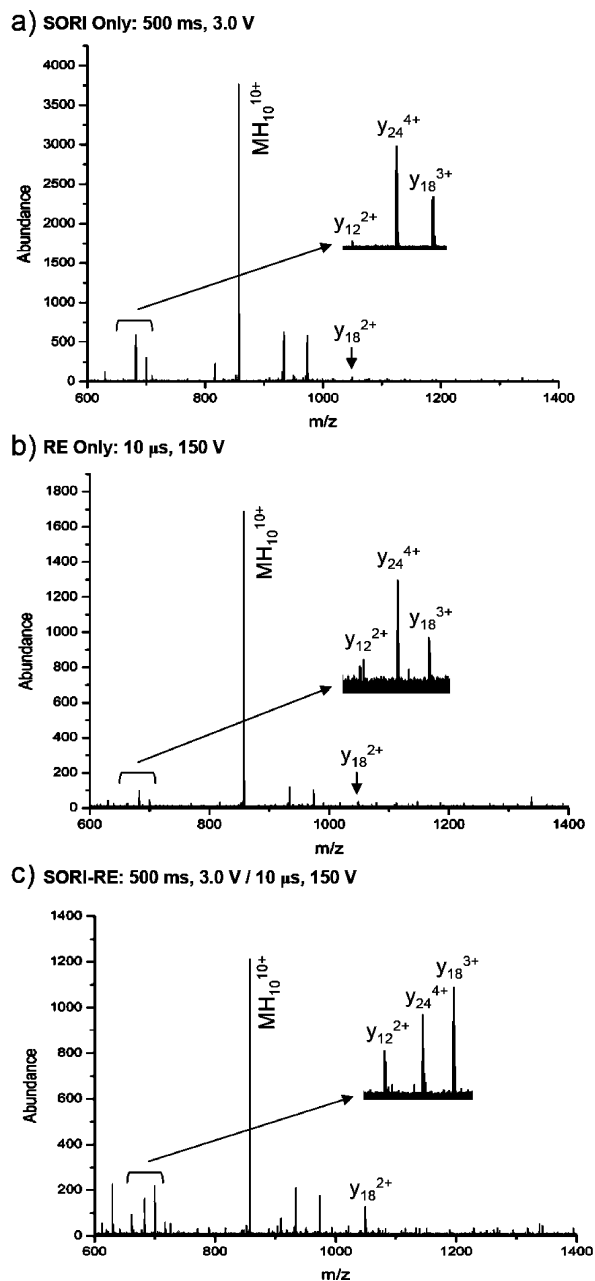


Figure 9. Fragmentation of the nonmonoisotopically selected [ubiquitin + 10H⁺]¹⁰⁺ ion using argon as the collision gas. (a) SORI: time 500 ms, amplitude 3.0 V. (b) RE: time 10 μ s, amplitude 150 V. (c) SORI-RE: SORI time 500 ms, amplitude 3.0 V, 20-ms time gap, RE time 10 μ s, amplitude 150 V.

example to demonstrate the changes in MS/MS spectra produced by SORI, RE, and their combination, SORI-RE. Figure 10a–c shows the SORI, RE, and SORI-RE CID (Ar) fragmentation of the singly charged uranyl cation (UO_2^+ , m/z 270.0). This is a stable cation that requires relatively high SORI amplitude to fragment. A 5.0-V SORI excitation amplitude was needed in order to observe the fragments UO^+ (m/z 254.0) and U^+ (m/z 238.1) with the abundances shown in Figure 10a. Note that the abundance of UO^+ was always larger than that of U^+ even at a higher SORI voltage (7 V) at which the parent ion was completely depleted (data not shown). The application of a 10- μ s, 300-V RE pulse resulted in the same fragments but with different relative abundances (Figure 10b). This suggests that higher internal energy was deposited by

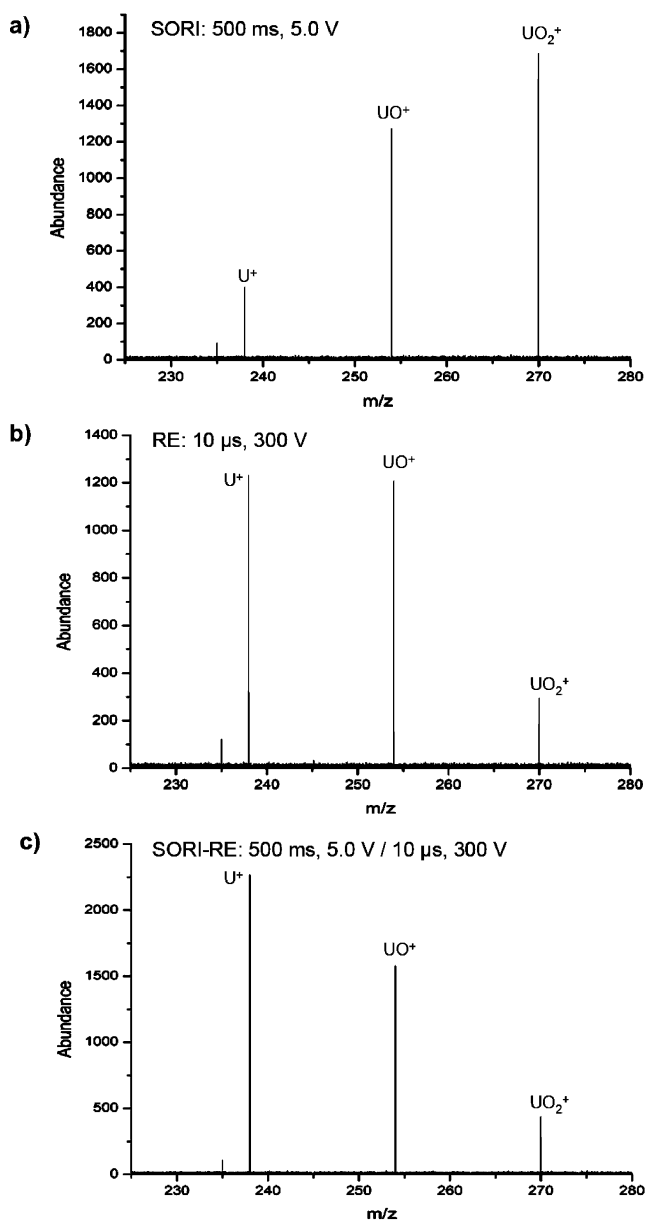


Figure 10. Fragmentation of the singly charged uranyl cation (UO_2^+) using argon as the collision gas. (a) SORI: time 500 ms, amplitude 5.0 V. (b) RE: time 10 μ s, amplitude 300 V. (c) SORI-RE: SORI time 500 ms, amplitude 5.0 V, 20-ms time gap, RE time 10 μ s, amplitude 300 V.

the RE pulse than by the SORI pulse. This energy deposition can be further increased when the SORI pulse is followed by the RE pulse (Figure 10c) as indicated by the reverse U^+/UO^+ (>1) abundance ratio.

CONCLUSIONS

SORI-RE CID is an excitation method for FT-ICR based on a combination of SORI and resonant excitation (RE). The purpose is to enhance higher energy fragmentation while maintaining low-energy processes. In addition, *relative* energy requirements of fragmentation mechanisms may be studied with this method. This concept is similar to the pump–probe experiments used to study fundamentals of collision energy transfer in FT-ICR.⁴⁰ SORI is applied initially to pump energy in small steps into the molecule

until a portion of the precursor ions dissociates while the remaining precursor ions maintain an internal energy below the fragmentation threshold. For large molecules (i.e., greater than 10 kDa), this fragmentation threshold may be far higher than the activation energy. Shortly following the SORI pulse (20-ms gap), a RE pulse is applied that increases the internal energy of the remaining activated but undissociated precursor ions significantly above the fragmentation threshold by also pumping energy into the activated molecules, but in a larger step. As demonstrated in Figure 3, this makes it possible to raise the internal energy much higher than would be possible by SORI alone. Utilizing RE only, especially for large molecules, would not be efficient because all or most of the large energy step would be “wasted” to heat up the molecule from thermal energy to the fragmentation threshold. These theoretical expectations are supported by the experimental results, as described above. Illustrative SORI-RE CID fragmentation examples include the observation of high-energy immonium ions in large quantities for leucine enkephalin (Figure 1c) and the enhancement of cross-ring cleavages for 2 α -mannobiose and 3 α -mannobiose (Figure 7c,f). It is important to note that different fragment ions observed may be due to higher energy fragmentation as well as the conversion of heterogeneous populations to different protonated forms, conformations, or both. The interconversion of heterogeneous forms as it relates to the relative abundance of different fragment ions may also be mechanistically interesting.

One of the most important advantages of SORI-RE is its simplicity. It does not require hardware or software modification on existing FT-ICR instruments, and method optimization is very simple. The best results are obtained with a SORI precursor ion survival yield of ~40–90% and can be adjusted by varying either SORI excitation amplitude or excitation time. The RE pulse is applied shortly following SORI (i.e., 20-ms gap as required by the

hardware) with the collision gas still in the cell. The amplitude and duration of the RE pulse should be chosen so that a significant amount of fragmentation is observed without signal extinction. It is most efficient to determine the RE pulse amplitude at which the signal begins to be depleted and then use ~80% of that amplitude for the resonant excitation step of SORI-RE. The SORI-RE technique is also quite robust: using a standard setup, typically both low and higher energy fragments are observed. In our experience, time-consuming experiment optimization is usually NOT required. Adding a “standard” RE pulse after the SORI cycle has a high probability of improving the MS/MS spectra.

The results discussed in the paper serve to illustrate the usefulness of SORI-RE in diverse cases: peptides (leucine enkephalin, an extensively studied model peptide), disaccharides with differing glycosidic linkages (2 α -mannobiose and 3 α -mannobiose), oligosaccharides (Alditol XT), proteins (ubiquitin), and inorganic ions (UO₂⁺). In each studied case, SORI-RE, compared to simple SORI, has been shown to enhance higher energy fragmentation processes.

ACKNOWLEDGMENT

This research was supported by NIH grant R01 GM051387 to V.H.W. This work was also supported by the Hungarian Research Fund (OTKA) T 043538 and the QLK2-CT-2002-90436 project of the European Union for Center of Excellence in Biomolecular Chemistry. The authors thank the Carlito Lebrilla research group at the University of California, Davis for providing the alditol XT sample.

Received for review May 12, 2005. Accepted September 8, 2005.

AC050828+